electronics

Article

Limitations of Multi-GNSS Positioning of USV in Area with High Harbour Infrastructure

Artur Makar

Department of Navigation and Hydrography, Polish Naval Academy, Smidowicza 69, 81-127 Gdynia, Poland; artur.makar@amw.gdynia.pl

Abstract: Satellite surveying techniques are currently among the main measuring technologies in geodesy and the main technologies in navigation. Modern navigation requires high accuracy of position coordinate determination, particularly in bathymetric surveys and aerial photogrammetry. In most cases, the terrain conditions enable positioning with high accuracy and reliability. These particularly involve the terrain conditions, i.e., high harbour infrastructure for bathymetric surveys and trees for railway surveys that hinder the measurement performance with a pre-determined accuracy. This article presents the limitations in unmanned survey vehicle (USV) positioning in an area restricted by a high quay, and difficult observational conditions in the surrounding high harbour infrastructure. The positioning used a four-system receiver that determined position coordinates based on the signals from one, two, three and four satellite navigation systems. The number of available satellites was determined under conditions of the open upper hemisphere and the partially obscured hemisphere based on the surrounding geometry. The determined position coordinates were related to the position determined using robotic total station (RTS). An area was identified in which it becomes difficult or impossible to maintain the required positioning accuracy.

Keywords: bathymetric surveys; unmanned survey vehicle (USV); multi-global navigation satellite system (multi-GNSS); satellite system; line keeping

Citation: Makar, A. Limitations of Multi-GNSS Positioning of USV in Area with High Harbour Infrastructure. *Electronics* **2023**, *12*, 697. https://doi.org/10.3390/electronics12030697

Academic Editors: Kannadhasan Suriyan, R. Nagarajan and George Ghinea

Received: 21 December 2022
Revised: 17 January 2023
Accepted: 29 January 2023
Published: 30 January 2023

1. Introduction

Bathymetric surveys, being one of the elements of hydrographic surveys [1,2], involve the determination of geospatial coordinates of a point cloud found on the bottom of the studied water region. Modern depth measurement techniques use acoustic waves emitted by the echo sounder transducer. Technological progress has popularised multibeam (MBES) and interferometric echosounders, but singlebeam echosounders (SBES) continue to be used due to their small size and weight.

The SBES bathymetric sounding technique involves guiding a sounding vessel along survey lines according to a determined, systematic pattern. These are usually parallel survey lines with a pre-determined distance between them. Thanks to the use of USVs [3–10], especially in the automatic mode of unit guiding along the survey lines, the efficiency of surveys (the speed of performance with an assumed level of detail) is much higher than for a sounding carried out using a hydrographic motorboat in a manual mode. Moreover, the accuracy of guiding a USV is much higher than that of guiding a motorboat [11–13].

Both the accuracy of guiding a survey vessel and the accuracy (reliability) of a bathymetric sounding [14,15] are determined, inter alia, by the accuracy of position coordinate determination using a global navigation satellite system (GNSS) receiver. In the littoral zone and harbour basins, geodetic receivers, which provide a coordinate determination accuracy of 2 cm (p = 95%) in dynamics [16–18], are used. The key factors determining the accuracy, availability, and continuity of position coordinate determination include the type of GNSS system, the number of visible satellites, the terrain conditions and the operation mode of the real time kinematic/network RTK/RTN correction transmission system.

Multi-system receivers [19–22] are available in the market for measuring receivers, including surveying receivers. The earliest receivers enabled the determination of position coordinates based on the signals transmitted by global positioning system (GPS) and globalnaja nawigacionnaja sputnikowaja sistiema (GLONASS) system satellites. As new satellite radio navigation systems were implemented, they were extended to be able to receive signals from Galileo and Beidou satellites. The current status of the autonomous navigation system constellations is presented in Table 1 [23].

Table 1. The current status of the autonomous navigation system constellation.

Type of System	Constellation Status		Type of Orbit			
	Current Number of Satellites	Number of Operational Satellites	MEO	GEO	GSO	IGSO
GPS	34	30	34	-	-	-
GLONASS	26	23	26	-	-	-
Beidou	48	42	28	8	-	12
Galileo	26	22	26	-	-	-
IRNSS [1]	8	7	-	3	-	5
QZSS [2]	4	4	-	1	3	-
Total satellites	146	128	114	12	3	17

[1] IRNSS- Indian Regional Navigational Satellite System, [2] QZSS—Quasi-Zenith Satellite System.

It is obvious that only certain systems are operational in a selected area, not all satellites are visible to the receiver antenna, or the reference correction service supports only certain GNSS systems–particularly in restricted, harbour water regions, where the upper hemisphere is limited by high quays and breakwaters as well as harbour infrastructure buildings. In addition, it causes a reduction in the number of visible satellites and the reception of signals reflected from buildings [24–32]. It appears that the increased number of satellites due to the application of a few satellite systems fails to provide the required positioning accuracy. This phenomenon is detrimental in terms of the reliability of digital sea bottom model (DSBM) determination and hazardous to USV guiding in automatic mode.

Positioning studies and surveys under difficult observational conditions are mainly carried out in geodesy (static) [33–37] and when using moving wheeled and rail vehicles (dynamic). Geodetic receivers are used in engineering measurements in urbanised areas in which high buildings constrain both the upper hemisphere and the satellite visibility. Where surveys are carried out under conditions of total sky obscuration, non-satellite methods, e.g., laser methods like total station (TS) [38–42] or RTS [43–47], integration of INS (Inertial Navigation System)/GNSS or INS/GPS [48–50], INS/GNSS/CNS (celestial navigation system) [51–56], and SINS (Strapdown Inertial Navigation system)/GPS/SAR (Synthetic Aperture Radar) [57,58] are used. Dynamic surveys involve the positioning of wheeled vehicles moving in the city, currently oriented towards autonomous vehicles [59–61] and rail vehicles, e.g., moving in a forest area [62–64]. For some, continuous positioning in time and space is important (wheeled vehicles), while for the others, it is possible to plan a surveying campaign to secure the positioning in time (geodetic surveys, positioning of rail vehicles, e.g., to determine the track axis [23,65]).

Publicly available applications have been developed for the planning of a surveying campaign, e.g., Trimble Planning [66], SKYPLOT DEM–software described in [67], SatNav Toolbox—a chargeable package for MATLAB (manufactured by The MathWorks, Natick, MA, USA) (paid toolkit for the MATLAB package), GeoPAL, i.e., software described on the EUSPA website [68]. For the assumed conditions of mask location and elevation, they enable the determination of satellite constellations above the receiver in a specified time with complete visibility of the sky and to select the optimal time interval to carry out the surveys. This is troublesome during dynamic surveys, as it necessitates introducing a break. Therefore, most of the railway surveys are carried out at night, when the rail vehicle traffic was reduced.

The time optimisation of USV bathymetric surveys in the coastal and restricted region is largely based on the hydrometeorological forecast. Factors such as wind direction and strength as well as the water level are taken into account. The overall assessment of the possibility of performing a sounding operation is affected by the state of the sea, wind parameters and the roll, pitch and heave [69–75]. A sounding boundary in shallow water can be estimated based on the forecast water level. Additional factors that hinder the performance of a sounding in a restricted water region include large vessels moored at harbour and shipyard quays as well as high quays and buildings. These make it difficult or impossible to position a surveying unit using a GNSS receiver.

The current article results from experience in hydrographic surveys in hard-to-reach water regions, positioning problems, and attempts to solve them to ensure the continuity of dynamic surveys on water. The article is structured as follows: Section 2 describes the surveyed water region, and the methodology for bathymetric sounding in a restricted water region. It also presents the surveying unit, and the positioning system used during the surveys. Section 3 presents the results of USV positioning surveys carried out in the automatic navigation mode along the survey lines. Both single- and multi-system GNSS positioning were used to analyse the number of visible satellites and the positioning accuracy, and to assess the possibility of sounding operation performance. Section 4 analyses the available number of satellites of particular systems and the cumulative number in a multi-system variant of the receiver operation, and determines the shadowing zone and the reduced number of satellites. It also analyses the horizontal root mean square (HRMS) and the positioning solution. The charts are presented in the universal transverse Mercator UTM 34N coordinate system and they contain a geographic grid in the world geodetic system WGS84.

2. Materials and Methods

2.1. Study Area

Marina Yacht Park is a modern marina that has been enhancing the attractiveness of the Polish Baltic coast since 2019. It is located in the city of Gdynia, on the Gulf of Gdańsk. The facility is equipped with functional resources tailored to the needs of the most demanding yachtspeople, and the modern management and booking system makes the Marina Yacht Park an ideal place prepared to accommodate vessels from Poland and abroad, and is friendly to regular shipowners [76].

The Marina Yacht Park offers 120 mooring places with access to water and electricity and perfectly prepared infrastructure. 72 mooring places are intended for vessels shorter than 14 m (10 A), 42 places for vessels shorter than 12 m, and six places for vessels shorter than 10 m. The marina depth allows vessels with a draught of up to 8 m to be accommodated [76]. On its southern side, it is surrounded by the President's Basin at which the ORP Błyskawica museum ship and the Dar Pomorza sailing ship are moored. On the western and northern sides, the quays are filled with residential infrastructure, including the SeaTowers comprising two skyscrapers with a height of 141.6 m, and the Yacht Park complex of luxury apartment buildings (Figure 1).

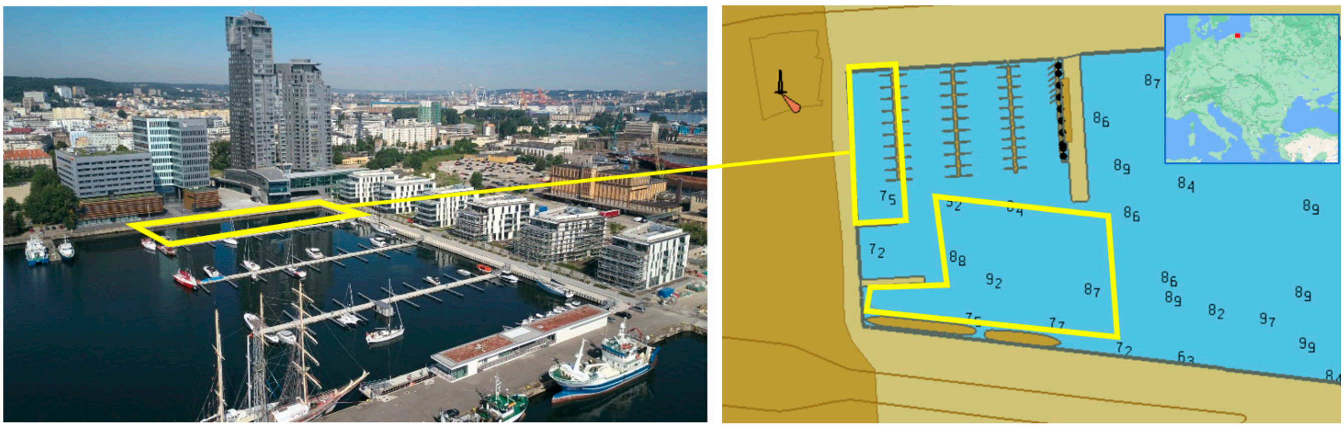

(**a**) (**b**)

Figure 1. Area of the study: (**a**) view on Marina Yacht Park [77]; (**b**) chart of the marina and President's Basin.

2.2. Bathymetric Measurements in Restricted Areas

In coastal water regions, the basic survey lines are designed perpendicular to the bottom relief course, the general direction of the isobaths, or the coastline. Control survey lines are designed perpendicular to the basic survey lines. In water regions with a varied coastline, the basic survey lines are designed at a 45° angle to the general direction of the contour lines or the coastline [1,2].

In the area of marine hydro-engineering structures, the basic survey lines are designed parallel to the course of the hydro-engineering structure. Control survey lines are designed perpendicular to the basic survey lines [1,2].

The densification of survey lines is used for surveys using SBES in order to more accurately determine the course of isobaths, and the bottom relief forms. To this end, additional survey lines are established in locations with signs of shoals and shallow water areas; in water regions where the depth and bottom relief vary significantly; in locations where the directions of the planned survey lines are close to the contour line course directions, which hinders their correct plotting; and on the canal and fairway axes [1,2].

The use of a USV enables the performance of bathymetric surveys with great detail (a short distance between survey lines) thanks to their small size, low sounding speed, high manoeuvrability and automatic navigation along the survey line. While the distance between survey lines for a sounding performed using a hydrographic motorboat has been 5–10 m, it is possible (for a sounding performed using a USV) to plan survey lines at a distance of 2 m, or even 1 m, between each other. Figure 2 shows the arrangement of survey lines for the sounding of Marina Yacht Park at a distance of 2 m between each other. The aim of the surveys was to determine the positioning capability of a sounding vessel under conditions of upper hemisphere obscuration by residential buildings and two Sea Towers buildings, and to determine a dead band for GNSS surveys.

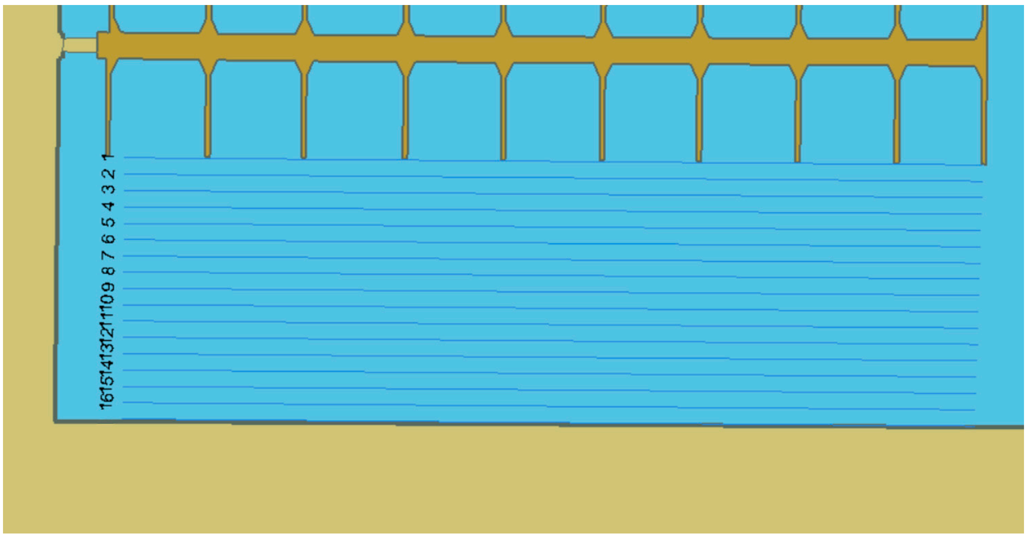

Figure 2. Survey lines in the area od study.

2.3. Equipment: USV and GNSS Receiver

Bathymetric surveys are carried out using a twin-engine USV OceanAlpha USV SL20 (OceanAlpha Group Ltd., Hong Kong, China) equipped with a single beam echosounder and an internal GPS receiver (Figure 3). In order to provide high accuracy of position coordinated measurement, the connection of an external GNSS receiver is enabled. It is located above the echo sounder transducer, which allows the coordinates of acoustic wave reflection from the bottom to be determined without transforming the position in the horizontal plane. The surveying unit is controlled remotely in either a manual or automatic mode after loading survey lines to its control system. Survey line planning, position control, and geospatial data recording during a bathymetric sounding operation are carried out in the HYPACK (HYPACK, Middletown, CT, USA)system onshore, thanks to two-way telemetric transmission.

Figure 3. USV OceanAlpha SL20.

Technical specification of the OceanAlpha USV SL20 is shown in Table 2.

Table 2. Technical specification of the OceanAlpha USV SL20.

Parameter	OceanAlpha USV SL20
Hull material	Carbon fiber
Dimension	105 cm × 55 cm × 35 cm
Weight	17 kg
Payload	8 kg
Draft	15 cm
Propulsion	water-jet propulsion
Communication range	Autopilot: 2 km Remote Control: 1 km
Remote control frequency	900 MHz/2.4 GHz
Data telemetry frequency	2.4 GHz/5.8 GHz
Survey speed	2–5 kn (1–2.5 m/s)
Max speed	10 kn (5 m/s)
Battery	6 h (1.5 m/s), 1 × 33 V 40 Ah
Positioning (standard—not used)	u-blox LEA-6 series
Positioning (used in maneuvering)	Topcon HiPer VR
Heading	Honeywell HMC6343
Echosounder	Echologger series SBES

Precise positioning is carried out using a multi-GNSS receiver, usually a dual-system Leica Viva or Topcon HiPer II (GPS + GLONASS), or a multi-system Topcon HiPer VR. The parameters of the Topcon HiPer VR receiver used for the study in a water region restricted by high shore infrastructure are shown in Table 3.

Table 3. Basic parameters of Topcon HiPer VR receiver.

GNSS Tracking	
Number of Channels	226 with Topcon's patented Universal Tracking Channels™ technology.
GPS [1]	L1 C/A, L1C [1] L2C, L2P(Y), L5
GLONASS [2]	L1 C/A, L1P, L2C/A, L2P, L3C [2]
Galileo	E1/E5a/E5b/Alt-BOC
Beidou	B1, B2
IRNSS	L5
QZSS	L1 C/A, L1C, L1-SAIF, L2C, L5
SBAS [3]	WAAS, EGNOS, MSAS, GAGAN (L1/L5)
L-Band	TopNET Global D & C Corrections services
Positioning Performance	
Static, Fast-Static (L1/L2)	H: 3 mm + 0.4 ppm V: 5 mm + 0.5 ppm
RTK (L1/L2)	H: 5 mm + 0.5 ppm V: 10 mm + 0.8 ppm
Frequency	1–20 Hz
Data	
Protocols	TPS, RTCM SC104 ver 2.x, 3.x, MSM3, CMR/CMR+, BINEX
Communication	
Radiomodem (optional)	UHF (406–470 MHz)
GSM/GPRS (optional)	internal

[1] L1C when signal available. [2] L3C when signal available. [3] L5 when signal available.

Data transmission in the National Marine Electronics Association (NMEA) format enables sounding unit positioning in real-time, with visualisation on an electronic map as a component of the HYPACK hydrographic system in which geospatial data are recorded. At the same time, observations are recorded in an FC-5000/6000 controller using the Magnet Field software, which enables the export of such data as Target point, Time, Latitude, Longitude, **Northing**, **Easting**, Ellipsoidal height, Elevation, HRMS, VRMS, Codes, HDOP, VDOP, Solution Type, **Number of GPS**, **Number of GLONASS**, **Number of BDS**, **Number of Galileo**, Number of SBAS, Number of QZSS, SigmaX, SigmaY, SigmaZ, TiltX, TiltY, TiltZ, Heading and more, selected according to the user's needs [78,79]. An example of a data record is as follows:

1017,10:49:33,54.311507182,18.330007346,**6,044,236.007**,**341,432.100**,29.469,0.050,0.060,1.466, 2.268,1.731,FIXED,**3**,**2**,**3**,**7**,0,0,12.5259984625,1.5215873991,−57.0851981824

where the rectangular coordinates in the UTM34N system, and the number of GPS, GLONASS, Beidou, and Galileo satellites, are shown in bold.

2.4. Multi-GNSS Positioning

The Topcon HiPer VR receiver enables the determination of position coordinates using satellites of at least one system, with this system being GPS. Dual-system positioning uses the GPS system and one of the three other systems: GLONASS, Galileo or Beidou. Triple-system positioning uses two other systems in addition to GPS, while four-system positioning uses satellites of all supported systems. The dynamic study of USV positioning in the Yacht Port marina used the following satellite system combinations shown in Table 4.

Table 4. Combination of GNSS systems.

Number of Satellite Systems	System	Time of Survey [min]
1	GPS	12
2	GPS + GLONASS	13
3	GPS + GLONASS + Beidou	9
4	GPS + GLONASS + Beidou + Galileo	15

In order to ensure precise horizontal positioning, the TPI NETpro network with an RTK_MSM5 correction stream dedicated to all four satellite systems, which ensures, alongside the NET_MSM5, the accuracy of horizontal coordinate determination of 3 cm (p = 0.95). In this variant, the reference station is immovable. The nearest stations are located in Gdańsk (at a distance of 19 km) and Wejherowo (23 km). The RTK mode of operation with the reference station in Gdańsk was selected in order to avoid the automatic set up of a new virtual station in the RTN mode due to the movement of the receiver mounted on the USV.

3. Results

3.1. Positioning in Open Area

Bathymetric surveys under good observational conditions, i.e., with good visibility of the positioning system satellites and undisturbed transmission of a reference correction stream, ensure high reliability of the obtained geospatial data [14,15]. The accuracy of position coordinate determination exceeds the international [80,81] and national requirements [82], and the control of the USV in an automatic mode proceeds correctly (Figure 4).

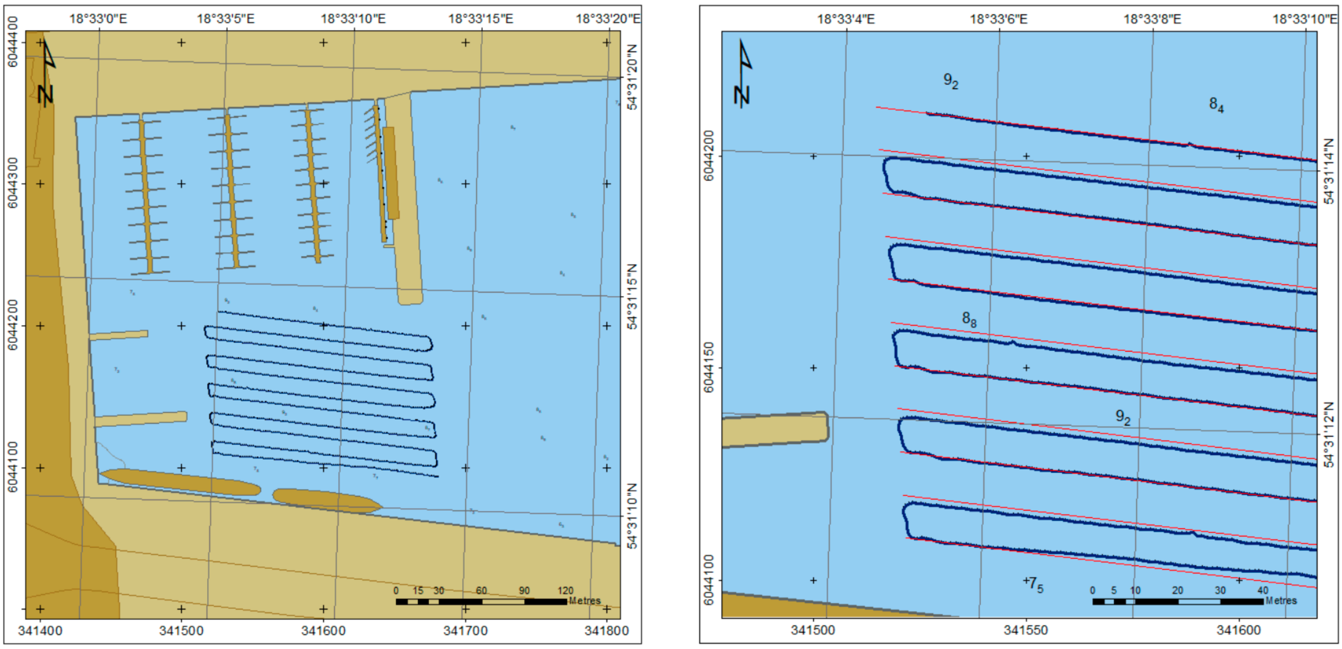

(**a**) (**b**)

Figure 4. USV trajectory in open area (**a**), trajectory in the background of survey lines (**b**).

The deviation of the current USV position from the planned survey line is small, i.e., no more than 1.5 m. It is determined in real-time, available to the operator in the hydrographic system HYPACK 2020, and used in the process of automated USV navigation. It can be calculated analytically as the distance of point P with rectangular plane coordinates of the GNSS system antenna (X_{POS},Y_{POS}) from the line on which lies the section which is a i-th survey line with the beginning (B) and end (E) coordinates [(X_{Bi},Y_{Bi}), (X_{Ei},Y_{Ei})]. Algoritm for determination the XTE parameter for USV OceanAlfa SL20 is described in [12].

3.2. GPS Positioning

Monitoring the USV trajectory on parallel survey lines commenced at a distance of 24 m from the quay in a southerly direction. After making a turn, the USV moved to the next survey line located at a distance of 2 m from the previous one. Each next survey line was located 2 m closer to the quay with high buildings. USV safety was monitored by the operator, including the possibility to switch from automatic to manual control in order to prevent USV damage when in contact with the quay. The trajectory determined using a GNSS receiver is marked in blue. The trajectory determined using RTS, whose prism was located directly under the GNSS receiver antenna, is marked in red. It can be seen that the deviation of the trajectory determined using a GNSS receiver deviated from the trajectory determined using RTS on three survey lines located closest to the quay (Figure 5a). 7–9 satellites were available (Figure 5b), which did not compromise the accuracy of coordinate determination.

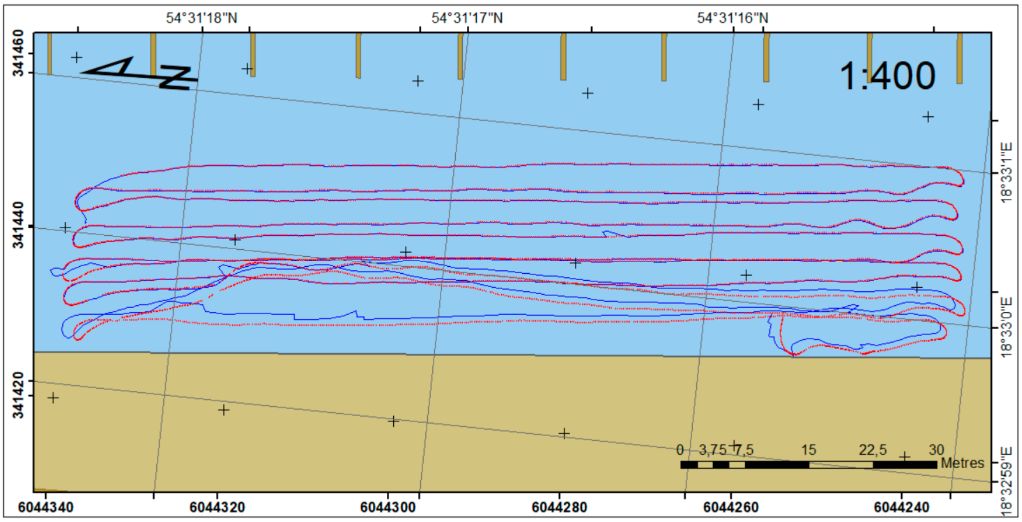

(**a**)

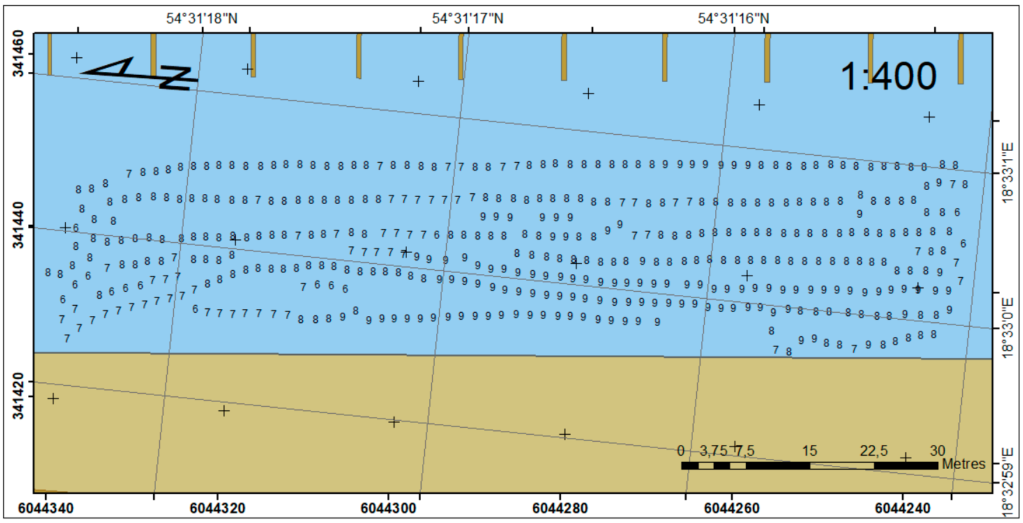

(**b**)

Figure 5. USV trajectory (**a**), total number of used satellites (**b**) for USV positioning (GPS only).

3.3. GPS + GLONASS Positioning

Thanks to the use of two systems (GPS and GLONASS), the number of available satellites almost doubled. Within the area marked in yellow (Figure 6a), the error of coordinate determination using a GNSS receiver was greater than 2.5 m, which exceeded the permissible error value specified for a special category (2 m) as defined in special publication S-44 [70]. On the survey lines located closest to the quay, the coordinate determination error oscillated around the value of 1 m with a momentary error of approx. 2.5 m at the end of the survey line. The number of visible satellites was 12–15, and locally dropped to 8–9 (Figure 6b).

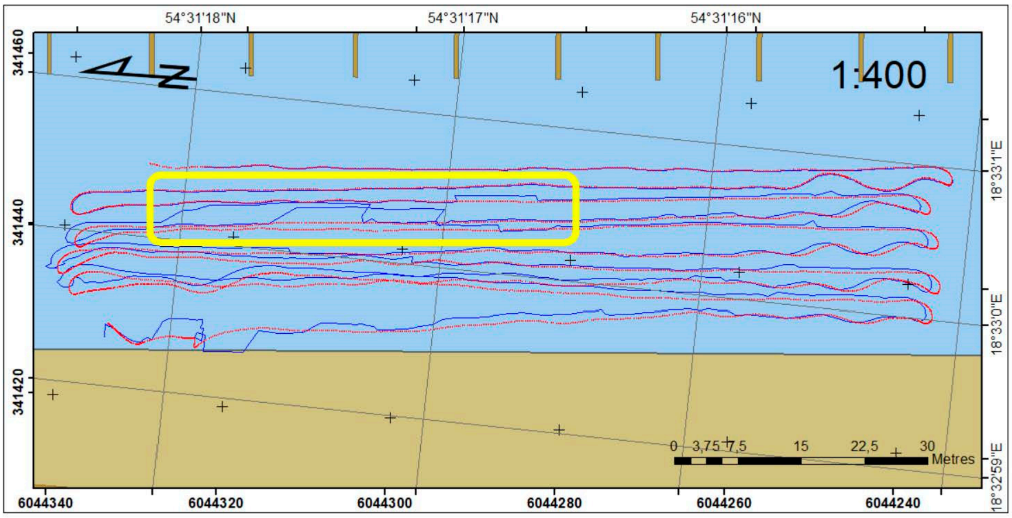

(**a**)

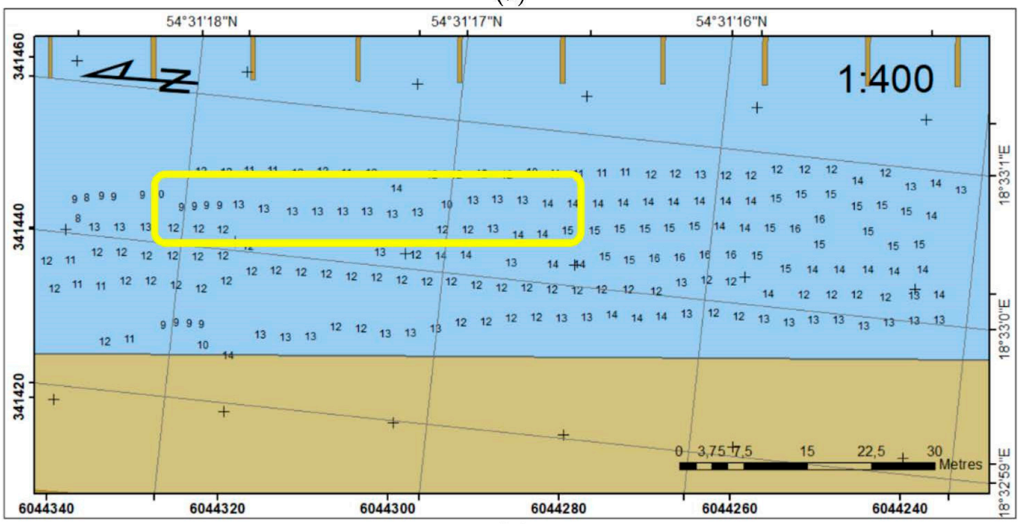

(**b**)

Figure 6. USV trajectory (**a**), total number of used satellites (**b**) for USV positioning (GPS + GLONASS).

3.4. GPS + GLONASS + Beidou Positioning

The third system used to increase the accuracy of USV positioning is Galileo. In a triple-system configuration, two deviations of the position determined using a GNSS receiver (Figure 7a), being a result of the loss of reception of satellite signals, can be observed. The number of available satellites from 20–23 to 7–10, or even 3 (Figure 7b).

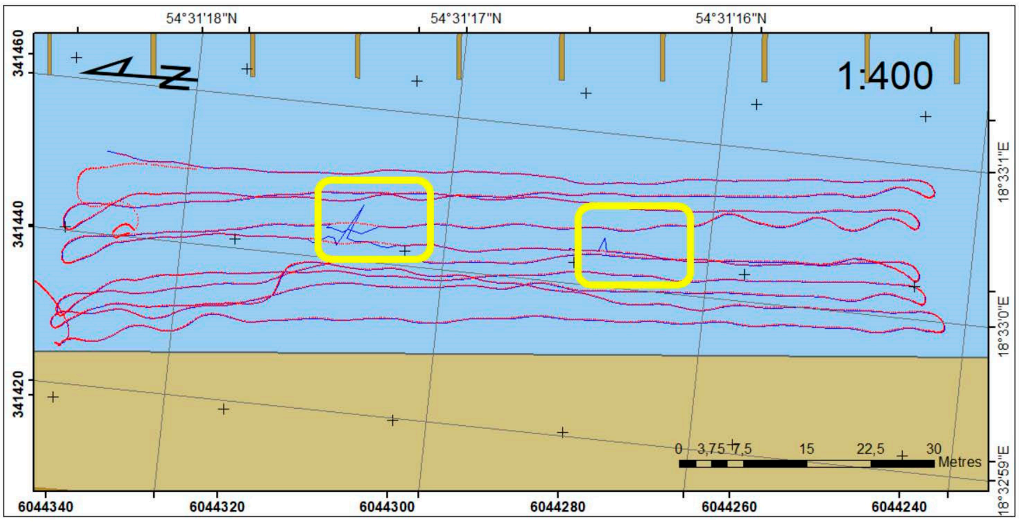

(**a**)

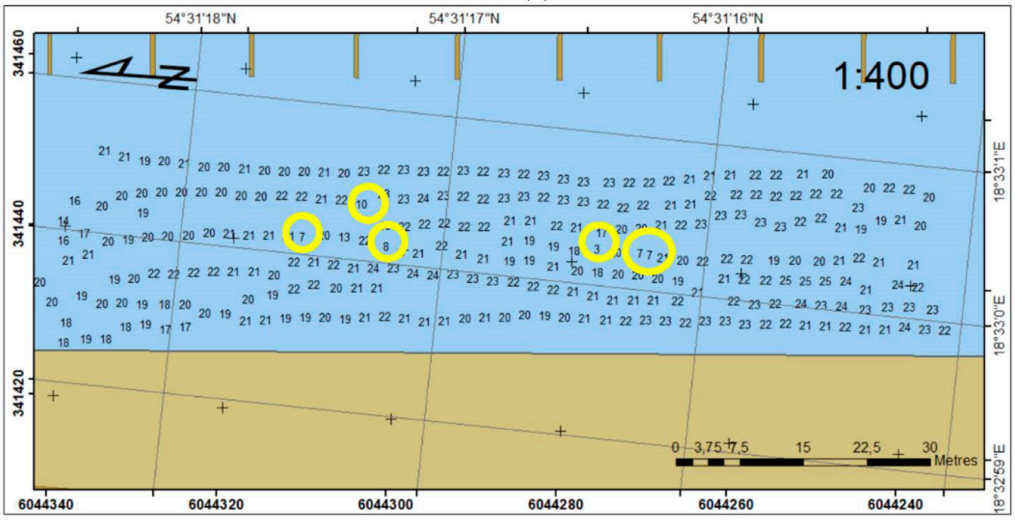

(**b**)

Figure 7. USV trajectory (**a**), total number of used satellites (**b**) for USV positioning (GPS + GLONASS + Beidou).

3.5. GPS + GLONASS + BeiDou + Galileo Positioning

The highest positioning accuracy was achieved using satellite signals of four systems for which TPI NETpro transmits corrections (Figure 8a). The minimum number of visible satellites is greater than 20 (Figure 8b), with no random or gross errors of the position coordinate determination noted. Similar to the triple-system variant (Section 3.5), a bathymetric sounding is performed on the survey lines located closest to the quay, which was not possible in the single- and dual-system variants.

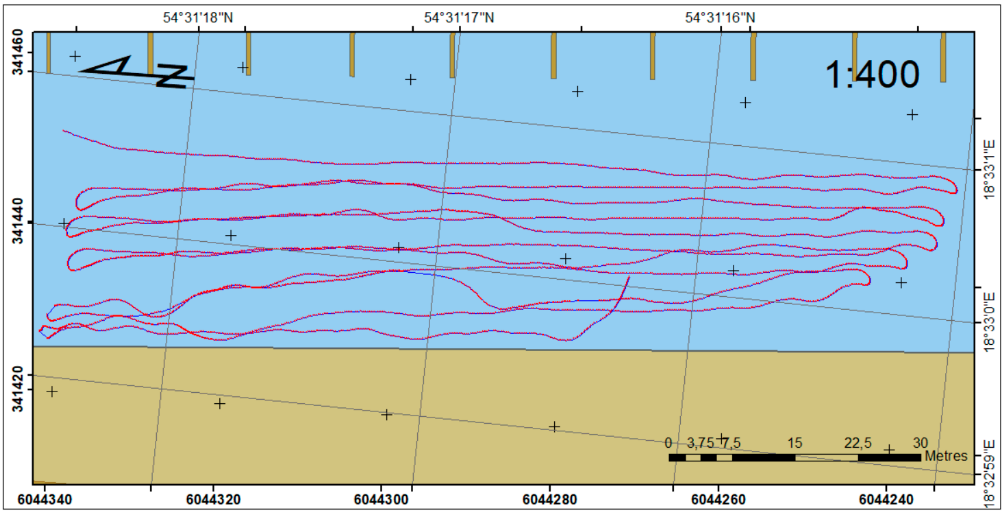

(**a**)

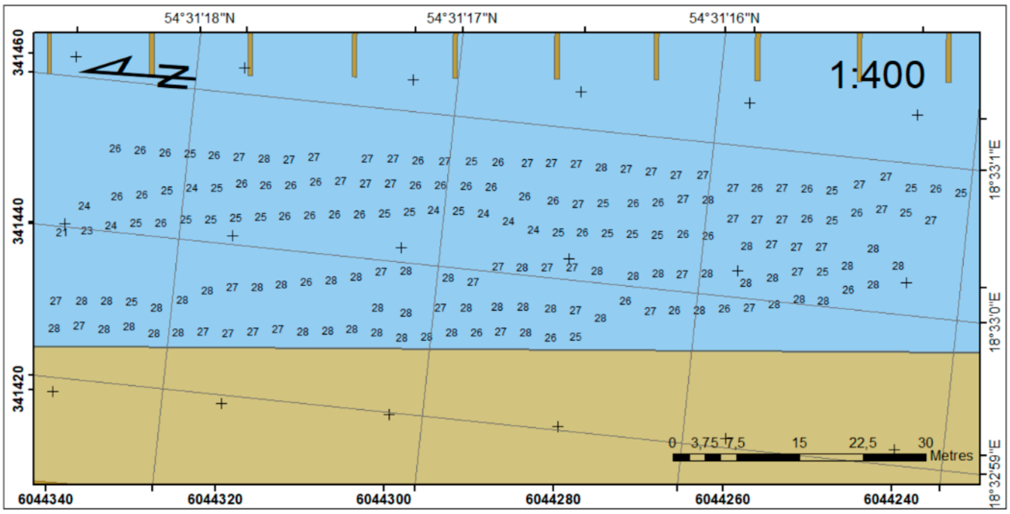

(**b**)

Figure 8. USV trajectory (**a**), total number of used satellites (**b**) for USV positioning (GPS + GLONASS + Beidou+ Galileo).

4. Discussion

4.1. Analyse of Satellites' Availability on the Basis of Trimble GNSS Planning

An analysis of GNSS satellite availability was conducted using the Trimble GNSS Planning [56] application available online, which enables the determination of the number of visible satellites for six systems. The analysis only used the systems for which the TPI NETpro network determined corrections. The Marina Yacht harbour basin was selected as the surveying location, and the surveying was performed at 12:15 to 13.45 on 24 July 2020. Due to the partial visibility of satellites above the horizon (the eastern part—the Gdynia harbour entrance) and low above the horizon (the southern part—the President's Basin), the elevation cut off angle of 10° was assumed). The sky plot for these conditions is shown in Figure 9a. To determine the sky obscuration, a spherical camera mounted on the USV was used (Figure 9b). On this basis and based on the chart, the area for which satellites would not be visible was determined (Figure 9c).

(**a**) (**b**) (**c**)

Figure 9. Sky plot with four systems satellites for 10° cut off angle (**a**), the view of the upper hemisphere by USV using spherical camera (**b**), sky plot with satellites visible by USV (**c**).

In Figure 10 are presented the number of satellites of individual GNSS system (left column) and total number of satellites in cumulated form.

GPS

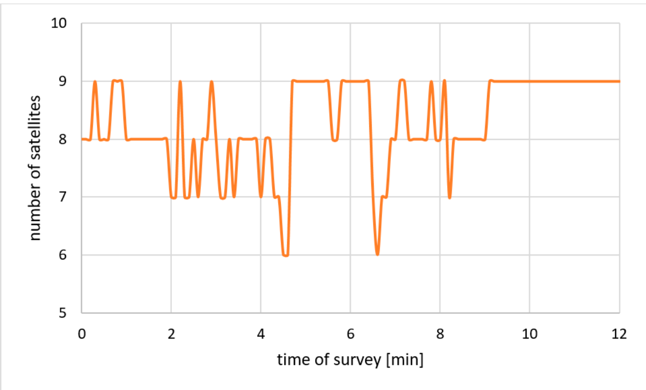

(**a**)

GPS/GLONASS

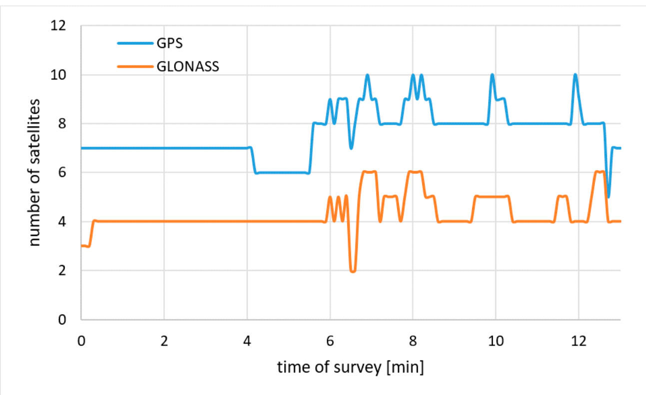

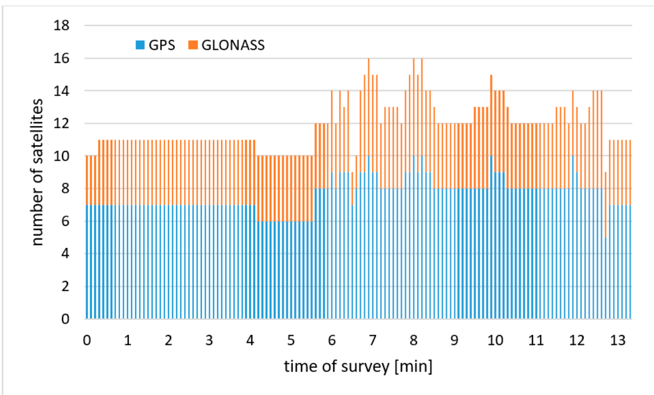

(**b**) (**c**)

Figure 10. *Cont.*

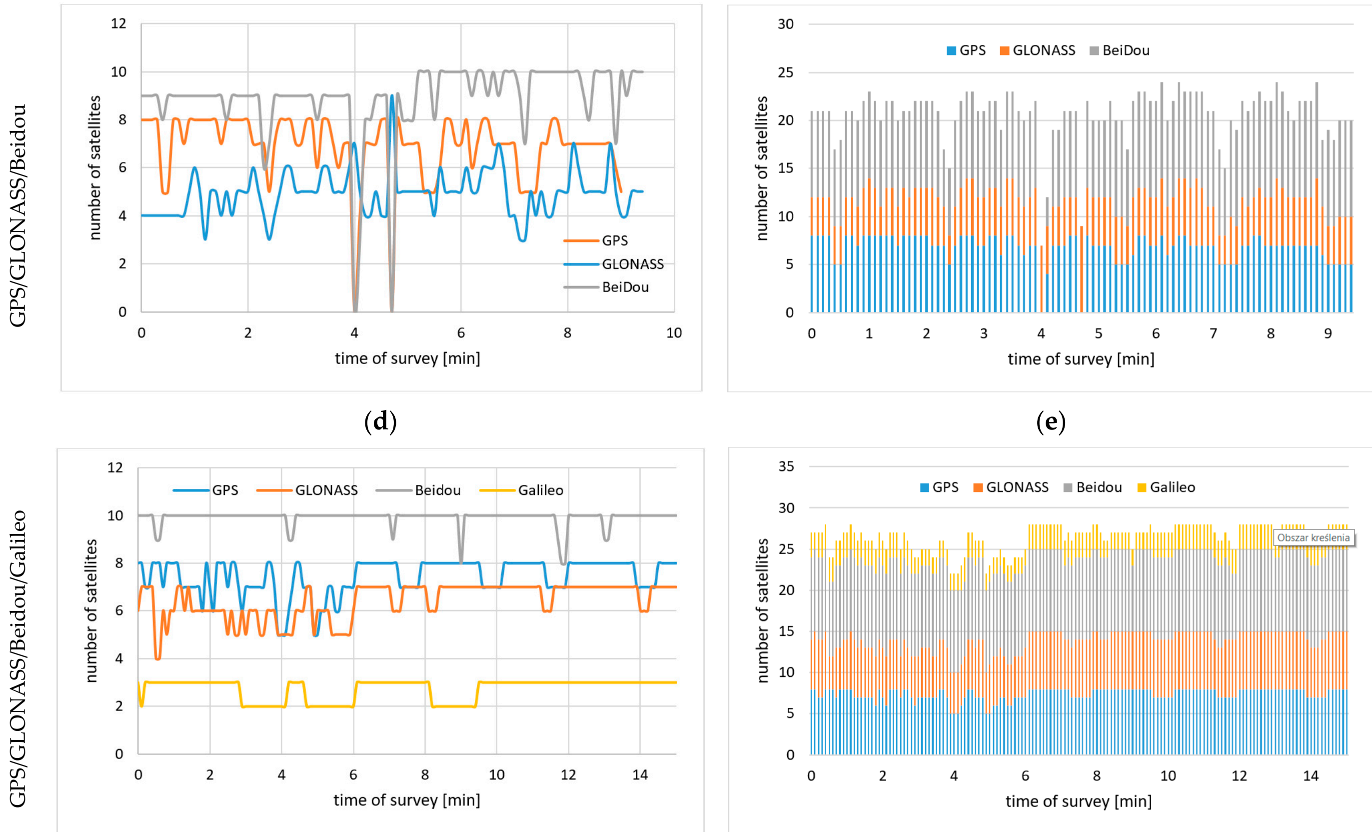

(**d**) (**e**)

(**f**) (**g**)

Figure 10. Individual (**a**,**b**,**d**,**f**) and cumulated (**c**,**e**,**g**) number of visible satellites.

Table 5 shows the number of satellites available in the surveyed water region during the performance of surveys, the number reduced by cutting off part of the upper hemisphere with harbour buildings, and the number recorded using a Topcon HiPer VR receiver during last survey (four systems).

Table 5. Number of available satellites.

System	Upper Hemisphere		Real
	Open	Reduced	
GPS	9	6	5–8
GLONASS	8	4	4–7
Beidou	12	11	9–10
Galileo	5	3	2–3
Total	34	24	20–28

During the positioning of a sounding unit on water, important indicators of the position coordinate determination accuracy include horizontal dilution of position (HDOP) and HRMS. The HDOP coefficient is determined in the Trimble Planner application for the pre-defined observational conditions. It is also available in NMEA messages and, along with the horizontal accuracy, in the files containing observational data recorded in the GNSS receiver controller (Table 6).

Table 6. HDOP.

System	Upper Hemisphere Open	Upper Hemisphere Reduced
GPS	1.15	2.83
GPS/GLONASS	0.71	1.65
GPS/GLONASS/Beidou	0.63	1.46
GPS/GLONASS/Beidou/Galileo	0.47	0.9

4.2. Continuity of Corrections and Positioning Solution

Depending on the number of satellites visible in the sky, it is possible to obtain a “float” or “fixed” positioning solution with different levels of accuracy. With a sufficient number of satellites visible, it can provide a fix position solution with centimetre accuracy. When not enough satellites are visible, the receiver can only provide a float solution with the best accuracy at that moment, which is not centimetre accurate. A lot of factors are taken into account to determine a “sufficient” number of satellites. A minimum of 12 satellite signals equally divided over the sky and a maximum base distance of 15 km, will get a fast and stable fix.

It was found in geodetic surveys (using a stationary receiver) that the fix-type solutions (with resolved indeterminacy of phase measurements) were characterised by a standard deviation within the limit of two centimetres, which corresponds to the theoretical accuracy of the RTK technique. In the group of float solutions (no resolved indeterminacy), the differences in coordinates fell within the limit of 1.5 m in the horizontal plane [25].

Dynamic surveys are characterised by a single measurement of the position coordinates. Due to the movement of the GNSS receiver antenna, it is not possible to determine the coordinates by averaging the results from several measurements. Moreover, in order to obtain highly detailed sounding results, the positioning frequency must be more than 1 Hz (5 or 10 Hz). Either only the data with the fix solution or all data (with the float and standalone solution) can be recorded. In the first case, the entire water region being sounded will not be covered with the recorded geospatial data. In the second case, the data will be affected by a horizontal error which often exceeds the required accuracies [71,73]. Figure 11 shows the HRMS value in relation to the positioning solution.

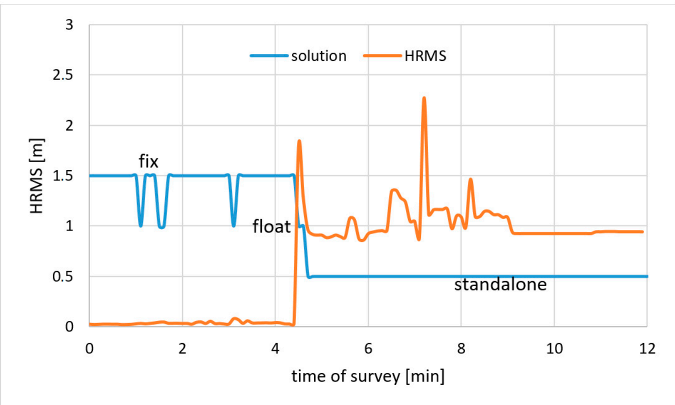

(**a**)

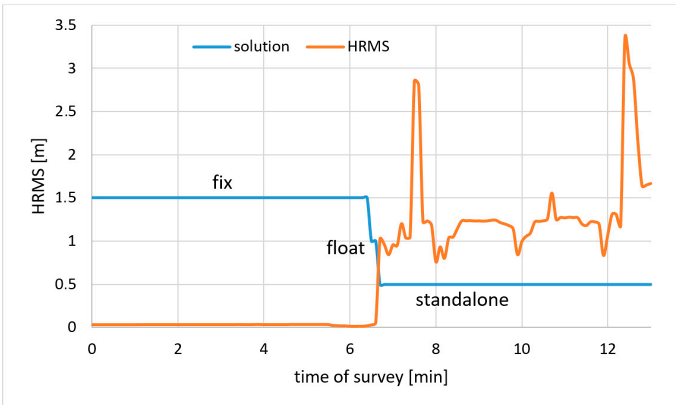

(**b**)

Figure 11. *Cont.*

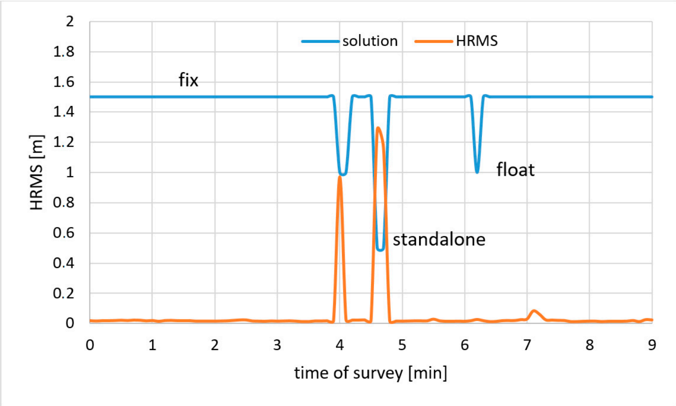

(**c**)

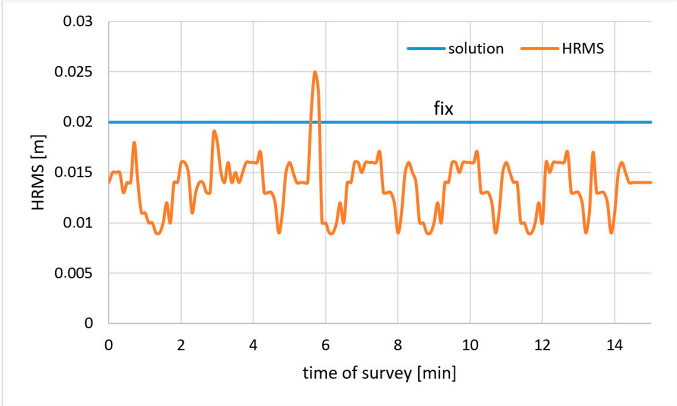

(**d**)

Figure 11. Positioning solution for 1—(**a**), 2—(**b**), 3—(**c**) and 4—(**d**) systems GNSS positioning.

In a single-system (GPS) and dual-system (GPS/GLONASS) variant of the GNSS receiver operation, the accuracy of position coordinate determination decreases drastically due to the lack of a fixed positioning solution. This phenomenon increasingly occurs on survey lines approaching the quay.

5. Conclusions

Precise positioning under dynamic conditions is the basis of bathymetric surveys. The methodology for planning survey lines and guiding a surveying unit along survey lines changes depending on the echo sounder used. For SBES, parallel survey lines are planned, and the helmsman's task is to maintain the surveying vessel on a survey line with a minimum XTE value. For a USV, the automatic navigation mode is the optimal solution (due to labour-intensiveness, time-consumption, and the accuracy of guiding the vessel along a survey line). Besides the direction measurement and autopilot, one of the factors affecting the accuracy of navigation along a survey line is positioning accuracy.

Under limited satellite visibility conditions, it is reasonable to use multi-system GNSS receivers. They determine the position coordinates from the total number of satellites seen by the receiver antenna. Under the conditions of the upper hemisphere open to the reception of signals from GNSS satellites, a lone single-system receiver is sufficient, while a dual-system receiver (commonly GPS/GLONASS) may prove insufficient under difficult observational conditions. The limitations for the use of such a receiver, with a sufficient number of satellites, include signal reflections from buildings or other large vessels (multipath) as well as the lack of a navigation solution ensuring the highest, one-centimetre accuracy of the position coordinate determination.

The aim of the article was to analyse the limitations in the positioning of a small USV sounding vessel based on the availability of GNSS system satellites in a water region restricted by high harbour buildings. Not only was the study aimed at ensuring high accuracy of the geospatial coordinate determination during a bathymetric sounding operation but also at keeping the USV in line in automatic navigation mode.

Funding: This research received no external funding.

Data Availability Statement: Not applicable.

Conflicts of Interest: The author declare no conflict of interest.

References

1. Hydrographic Office of the Polish Navy. *Maritime Hydrography—Organization and Research Rules*; Hydrographic Office of the Polish Navy: Gdynia, Poland, 2009.
2. Hydrographic Office of the Polish Navy. *Maritime Hydrography—Rules of Data Collecting and Results Presentation*; Hydrographic Office of the Polish Navy: Gdynia, Poland, 2009.

3. Stateczny, A.; Grońska, D.; Motyl, W. Hydrodron—New step for professional hydrography for restricted waters. In Proceedings of the 2018 Baltic Geodetic Congress, Olsztyn, Poland, 21–23 June 2018.
4. Specht, C.; Świtalski, E.; Specht, M. Application of an autonomous/unmanned survey vessel (ASV/USV) in bathymetric measurements. *Pol. Marit. Res.* **2017**, *24*, 36–44. [CrossRef]
5. Giordano, F.; Mattei, G.; Parente, C.; Peluso, F.; Santamaria, R. MicroVEGA (Micro Vessel for Geodetics Application): A Marine Drone for the Acquisition of Bathymetric Data for GIS Applications. *Int. Arch. Photogramm. Remote Sens. Spat. Inf. Sci.* **2015**, *40*, 123–130. [CrossRef]
6. Giordano, F.; Mattei, G.; Parente, C.; Peluso, F.; Santamaria, R. Integrating Sensors into a Marine Drone for Bathymetric 3D Surveys in Shallow Waters. *Sensors* **2016**, *16*, 41. [CrossRef] [PubMed]
7. Makar, A.; Specht, C.; Specht, M.; Dąbrowski, P.; Szafran, M. Integrated Geodetic and Hydrographic Measurements of the Yacht Port for Nautical Charts and Dynamic Spatial Presentation. *Geosciences* **2020**, *10*, 203. [CrossRef]
8. Makar, A. Determination of USV's Direction Using Satellite and Fluxgate Compasses and GNSS-RTK. *Sensors* **2022**, *22*, 7895. [CrossRef]
9. Romano, A.; Duranti, P. Autonomous Unmanned Surface Vessels for Hydrographic Measurement and Environmental Monitoring. In Proceedings of the FIG Working Week 2012, Rome, Italy, 6–10 May 2012.
10. Liu, Z.; Zhang, Y.; Yu, X.; Yuan, C. Unmanned Surface Vehicles: An Overview of Developments and Challenges. *Annu. Rev. Control.* **2016**, *41*, 71–93. [CrossRef]
11. Makar, A. Determination of the Minimum Safe Distance between a USV and a Hydro-Engineering Structure in a Restricted Water Region Sounding. *Energies* **2022**, *15*, 2441. [CrossRef]
12. Stateczny, A.; Burdziakowski, P.; Najdecka, K.; Domagalska-Stateczna, B. Accuracy of Trajectory Tracking Based on Nonlinear Guidance Logic for Hydrographic Unmanned Surface Vessels. *Sensors* **2020**, *20*, 832. [CrossRef]
13. Mu, D.; Wang, G.; Fan, Y.; Qiu, B.; Sun, X. Adaptive Trajectory Tracking Control for Underactuated Unmanned Surface Vehicle Subject to Unknown Dynamics and Time-varing Disturbances. *Appl. Sci.* **2018**, *8*, 547. [CrossRef]
14. Makar, A. Verification of the Digital Sea Bottom Model Built by Bathymetric Data–Deep Water Study. In Proceedings of the International Conference on Geo Sciences GEOLINKS 2019, Athens, Greece, 26–29 March 2019; Volume 1, pp. 287–295.
15. Makar, A. Reliability of the Digital Sea Bottom Model Sourced by Multibeam Echosounder in Shallow Water. In Proceedings of the 5th World Multidisciplinary Earth Sciences Symposium WMESS, Prague, Czech Republic, 9–13 September 2019.
16. Makar, A. Dynamic Tests of ASG-EUPOS Receiver in Hydrographic Application. In Proceedings of the 18th International Multidisciplinary Scientific GeoConference SGEM, Albena, Bulgaria, 30 June–9 July 2018; Volume 18, pp. 743–750.
17. Specht, C.; Makar, A.; Specht, M. Availability of the GNSS geodetic networks position during the hydrographic surveys in the ports. *Transnav Int. J. Mar. Navig. Saf. Sea Transp.* **2018**, *12*, 657–661. [CrossRef]
18. Wang, L.; Li, Z.; Zhao, J.; Zhou, K.; Wang, Z.; Yuan, H. Smart Device-supported BDS/GNSS Real-time Kinematic Positioning for Sub-meter-level Accuracy in Urban Location-based Services. *Sensors* **2016**, *16*, 2201. [CrossRef]
19. Jiao, G.; Song, S.; Ge, Y.; Su, K.; Liu, Y. Assessment of BeiDou-3 and Multi-GNSS Precise Point Positioning Performance. *Sensors* **2019**, *19*, 2496. [CrossRef] [PubMed]
20. Lohan, E.S.; Borre, K. Accuracy Limits in Multi-GNSS. *IEEE Trans. Aerosp. Electron. Syst.* **2017**, *52*, 2477–2494. [CrossRef]
21. Jang, W.S.; Park, H.S.; Seo, K.Y.; Kim, Y.K. Analysis of positioning accuracy using multi differential GNSS in coast and port area of South Korea. *J. Coast. Res.* **2016**, *75*, 1337–1341. [CrossRef]
22. Ziquan, H.; Xiufeng, H.; Liu, Z.; Sang, W. Analysis of the DOP Values and Availability of Combined GPS/GLONASS/GALILEO Navigation System. *GNSS World China* **2012**, *37*, 32–37.
23. Figiel, S.; Specht, C.; Moszyński, M.; Stateczny, A.; Specht, M. Testing of Software for the Planning of a Linear Object GNSS Measurement Campaign under Simulated Conditions. *Energies* **2021**, *14*, 7896. [CrossRef]
24. Ciećko, A.; Maliszewski, P. Analysis of Availability and Accuracy of Real-Time GPS/GLONASS Positioning in Difficult Observation Conditions. *Logistyka* **2011**, *6*, 525–535.
25. Hussain, A.; Akhtar, F.; Khand, Z.H.; Rajput, A.; Shaukat, Z. Complexity and Limitations of GNSS Signal Reception in Highly Obstructed Enviroments. *Eng. Technol. Appl. Sci. Res.* **2021**, *2*, 6864–6868. [CrossRef]
26. Jin, S. *Global Navigation Satellite Systems: Signal, Theory and Applications*; IntechOpen: London, UK, 2012. [CrossRef]
27. Dammalage, T.L. The Effect of Multipath on Single Frequency C/A Code Based GPS Positioning. *Eng. Tech. App. Sci. Res.* **2018**, *4*, 3270–3275. [CrossRef]
28. Error Sources, Novatel. 2015. Available online: https://novatel.com/an-introduction-to-gnss/chapter-4-gnsserror-sources/error-sources (accessed on 31 December 2021).
29. Zhang, Z.; Li, B.; Gao, Y.; Shen, Y. Real-time carrier phase multipath detection based on dual-frequency C/N0 data. *GPS Sol.* **2019**, *23*, 7. [CrossRef]
30. Xie, P.; Petovello, M.G. Measuring GNSS Multipath Distributions in Urban Canyon Environments. *IEEE Trans. Instr. Meas.* **2015**, *2*, 366–377. [CrossRef]
31. Suzuki, T. Mobile robot localization with GNSS multipath detection using pseudorange residuals. *Adv. Rob.* **2019**, *12*, 602–613. [CrossRef]
32. Hasan, M.; Rouf, R.R.; Islam, S. Investigation of Most Ideal GNSS Framework (GPS, GLONASS and GALILEO) for Asia Pacific Region (Bangladesh). *Int. J. Appl. Inf. Syst.* **2017**, *12*, 33–37. [CrossRef]

33. Bakuła, M.; Oszczak, S.; Pelc-Mieczkowska, R. Performance of RTK positioning in forest conditions: Case study. *J. Surv. Eng.* **2009**, *3*, 125–130. [CrossRef]
34. Bakuła, M.; Oszczak, S. Experiences of RTK positioning in hard observational conditions during Nysa Kłodzka river Project. *Rep. Geod.* **2006**, *1*, 71–79.
35. Bakuła, M.; Pelc-Mieczkowska, R.; Walawski, M. Reliable and redundant RTK positioning for applications in hard observational conditions. *Artif. Satell.* **2012**, *47*, 23–33. [CrossRef]
36. Makar, A. Determination of Inland Areas Coastlines. In Proceedings of the 18th International Multidisciplinary Scientific GeoConference SGEM, Albena, Bulgaria, 2–8 July 2018; Volume 18, pp. 701–708.
37. Lee, I.; Ge, L. The performance of RTK-GPS for surveying under challenging environmental conditions. *Earth Planets Space* **2006**, *58*, 515–522. [CrossRef]
38. Walker, J.; Awange, J. Total Station: Measurements and Computations. In *Surveying for Civil and Mine Engineers*; Springer: Cham, Switzerland, 2020. [CrossRef]
39. Felski, A. Measuring the Speed of Docking Ship with Total Station. *Commun. Sci. Lett. Univ. Zilina* **2022**, *24*, E1–E10. [CrossRef]
40. Hussein, S.; Yaseen, K. Surveying with GNSS and Total Station: A Comparative Study. *Eurasian J. Sci. Eng.* **2021**, *7*, 59–73. [CrossRef]
41. Xu, Y.; Zhao, X.; Liu, H.; Xu, F.; Wang, X. The Improvement and application of elevation measurement method with total station. *E3S Web Conf.* **2020**, *165*, 03018. [CrossRef]
42. Alizadeh-Khameneh, M.A.; Horemuž, M.; Jensen, A.; Vium, A. Optimal Vertical Placement of Total Station. *J. Surv. Eng.* **2018**, 144. [CrossRef]
43. Pehlivan, H. The Analysis Methodology of Robotic Total Station Data for Determination of Structural Displacements. *Adv. Geom.* **2021**, *1*, 1–7.
44. Ditta, M.; Colson, A. Total Station Surveying. In *Digital Techniques for Documenting and Preserving Cultural Heritage*; Anna Bentkowska-Kafel, A., MacDonald, L., Eds.; Amsterdam University Press: Amsterdam, The Netherlands, 2018; pp. 253–256. [CrossRef]
45. Zhou, J.; Luo, C.; Jiang, W.; Yu, X.; Wang, P. Using UAVs and robotic total stations in determining height differences when crossing obstacles. *Measurement* **2021**, *188*, 110372. [CrossRef]
46. Psimoulis, P.; Stiros, S. Experimental assessment of the accuracy of GPS and RTS for the determination of the parameters of oscillation of major structures. *Comput. -Aided Civ. Infrastruct. Eng.* **2008**, *23*, 389–403. [CrossRef]
47. Psimoulis, P.; Stiros, S. Robotic Theodolites (RTS) Measuring Structure Excitation. *GIM Int.* **2011**, *25*, 29–33.
48. Hu, G.; Wang, W.; Zhong, Y.; Gao, B.; Gu, C. A new direct filtering approach to INS/GNSS integration. *Aerosp. Sci. Technol.* **2018**, *77*, 755–764. [CrossRef]
49. Meng, Y.; Gao, S.; Zhong, Y.; Hu, G.; Subic, A. Covariance matching based adaptive unscented Kalman filter for direct filtering in INS/GNSS integration. *Acta Astronaut.* **2016**, *120*, 171–181. [CrossRef]
50. Hu, G.; Gao, S.; Zhong, Y. A derivative UKF for tightly coupled INS/GPS integrated navigation. *ISA Trans.* **2015**, *56*, 135–144. [CrossRef]
51. Gao, B.; Hu, G.; Zhong, Y.; Zhu, X. Distributed State Fusion Using Sparse-Grid Quadrature Filter With Application to INS/CNS/GNSS Integration. *IEEE Sens. J.* **2022**, *22*, 3430–3441. [CrossRef]
52. Gao, B.; Hu, G.; Gao, S.; Zhong, Y.; Gu, C. Multi-sensor optimal data fusion for INS/GNSS/CNS integration based on unscented Kalman filter. *Int. J. Control. Autom. Syst.* **2018**, *16*, 129–140. [CrossRef]
53. Hu, G.; Gao, S.; Zhong, Y.; Gao, B.; Subic, A. Matrix weighted multisensor data fusion for INS/GNSS/CNS integration. *Proc. Inst. Mech. Eng. Part G J. Aerosp. Eng.* **2016**, *230*, 1011–1026. [CrossRef]
54. Hu, G.; Gao, S.; Zhong, Y.; Gao, B.; Subic, A. Modified federated Kalman filter for INS/GNSS/CNS integration. *J. Aerosp. Engineering* **2016**, *230*, 30–44. [CrossRef]
55. Gao, Z.; Mu, D.; Zhong, Y.; Gu, C. Constrained Unscented Particle Filter for SINS/GNSS/ADS Integrated Airship Navigation in the Presence of Wind Field Disturbance. *Sensors* **2019**, *19*, 471. [CrossRef] [PubMed]
56. Liao, M.; Liu, J.; Meng, Z.; You, Z. A SINS/SAR/GPS Fusion Positioning System Based on Sensor Credibility Evaluations. *Remote Sens.* **2021**, *13*, 4463. [CrossRef]
57. Gao, S.; Xue, L.; Zhong, Y.; Gu, C. Random weighting method for estimation of error characteristics in SINS/GPS/SAR integrated navigation system. *Aerosp. Sci. Technol.* **2015**, *46*, 22–29. [CrossRef]
58. Gao, S.; Zhong, Y.; Zhang, X.; Shirinzadeh, B. Multi-sensor optimal data fusion for INS/GPS/SAR integrated navigation system. *Aerosp. Sci. Technol.* **2009**, *13*, 232–237. [CrossRef]
59. Tanil, C.; Khanafseh, S.; Joerger, M.; Kujur, B.; Kruger, B.; de Groot, L.; Pervan, B. Optimal INS/GNSS Coupling for Autonomous Car Positioning Integrity. In Proceedings of the 32nd International Technical Meeting of the Satellite Division of The Institute of Navigation (ION GNSS+ 2019), Miami, FL, USA, 16–20 September 2019; pp. 3123–3140. [CrossRef]
60. Khanafseh, S.; Kujur, B.; Joerger, M.; Walter, T.; Pullen, S.; Blanch, J.; Doherty, K.; Norman, L.; de Groot, L.; Pervan, B. GNSS Multipath Error Modeling for Automotive Applications. In Proceedings of the 31st International Technical Meeting of the Satellite Division of The Institute of Navigation (ION GNSS+ 2018), Miami, FL, USA, 24–28 September 2018; pp. 1573–1589. [CrossRef]
61. Zhu, N.; Marais, J.; Bétaille, D.; Berbineau, M. GNSS Position Integrity in Urban Environments: A Review of Literature. *IEEE Trans. Intell. Transp. Syst.* **2018**, *19*, 2762–2778. [CrossRef]

62. Wilk, A.; Koc, W.; Specht, C.; Skibicki, J.; Judek, S.; Karwowski, K.; Chrostowski, P.; Szmagliński, J.; Dąbrowski, P.; Czaplewski, K.; et al. Innovative mobile method to determine railway track axis position in global coordinate system using position measurements performed with GNSS and fixed base of the measuring vehicle. *Measurement* **2021**, *175*, 109016. [CrossRef]
63. Specht, C.; Wilk, A.; Koc, W.; Karwowski, K.; Dąbrowski, P.; Specht, M.; Grulkowski, S.; Chrostowski, P.; Szmagliński, J.; Czaplewski, K.; et al. Verification of GNSS Measurements of the Railway Track Using Standard Techniques for Determining Coordinates. *Remote Sens.* **2020**, *12*, 2874. [CrossRef]
64. Koc, W.; Wilk, A.; Specht, C.; Karwowski, K.; Skibicki, J.; Czaplewski, K.; Judek, S.; Chrostowski, P.; Szmagliński, J.; Dąbrowski, P.; et al. Determining Horizontal Curvature of Railway Track Axis in Mobile Satellite Measurements. *Bull. Pol. Acad. Sci.* **2021**, *69*, e139204. [CrossRef]
65. Skóra, M. Optimize Campaign Mission Planning GNSS for Dynamic Measurements of Linear Objects. Ph.D. Dissertation, Polish Naval Academy, Gdynia, Poland, 2018. (In Polish).
66. Trimble GNSS Planning Online. Available online: https://www.gnssplanning.com (accessed on 15 December 2021).
67. Gandolfi, S.; La Via, L. SKYPLOT_DEM: A Tool for GNSS Planning and Simulations. *Appl. Geomat.* **2011**, *3*, 35–48. [CrossRef]
68. EUSPA. GeoPAL GNSS-based Planning System for Agricultural Logistics. Available online: https://www.euspa.europa.eu/gnss-based-planning-system-agricultural-logistics (accessed on 19 November 2021).
69. Hopkins, R.; Adamo, L. Heave-roll-pitch correction for hydrographic and multi-beam survey systems. *Ocean. Manag.* **1981**, *7*, 85–97. [CrossRef]
70. Work, P.; Hansen, M.; Rogers, W. Bathymetric Surveying with GPS and Heave, Pitch, and Roll Compensation. *J. Surv. Eng. ASCE* **1998**, *124*, 73–90. [CrossRef]
71. Küchler, S.; Eberharter, J.; Langer, K.; Schneider, K.; Sawodny, O. Heave Motion Estimation of a Vessel Using Acceleration Measurements. In Proceedings of the 18th IFAC World Congress, Milano, Italy, August 28–2 September 2011.
72. Barrass, C.B.; Derrett, D.R. Rolling, Pitching, and Heaving Motions. In *Ship Stability for Masters and Mates*, 7th ed.; Barrass, C.B., Derrett, D.R., Eds.; Butterworth-Heinemann: Oxford, UK, 2012; pp. 413–423. [CrossRef]
73. Dostal, L.; Kreuzer, E.; Sri Namachchivaya, N. Stochastic Averaging of Roll-Pitch and Roll-Heave Motion in Random Seas. *Procedia IUTAM* **2013**, *6*, 132–140. [CrossRef]
74. Zhou, X.; Li, H.; Huang, Y. Stochastic averaging for estimating a ship roll in random longitudinal or oblique waves. *Mar. Struct.* **2021**, *75*, 102814. [CrossRef]
75. Felski, A.; Naus, K.; Wąż, M. The Problem of the Instrument Stabilization during Hydrographic Measurements. *Rep. Geod. Geoinf.* **2016**, *100*, 55–65. [CrossRef]
76. Marina Yacht Park. Available online: https://www.marinayachtpark.pl/ (accessed on 1 November 2022).
77. DORACO. Available online: http://www.doraco.pl/en/portfolio/construction-of-gdynia-yacht-park-housing-estate-including-a-marina/ (accessed on 1 November 2022).
78. Topcon Positioning Systems, Inc. *MAGNET Field Help, Version 3.0*; Topcon Positioning Systems, Inc.: South Brisbane, QLD, Australia, 2015.
79. Topcon Positioning Systems, Inc. *HiPer VR GNSS Receiver Operator's Manual, Version 3.0*; Topcon Positioning Systems, Inc.: South Brisbane, QLD, Australia, 2015.
80. International Hydrographic Organization. *IHO Standards for Hydrographic Surveys*, 6th ed.; Special Publication No. 44; IHO: Monte Carlo, Monaco, 2018.
81. Canadian Hydrographic Service. *CHS Standards for Hydrographic Surveys*, 2nd ed.; CHS: Ottawa, ON, Canada, 2013.
82. Ministry of Defence of the Republic of Poland. *Act of 28 March 2018 on the Minimum Standards for Hydrographic Surveys*; Ministry of Defence of the Republic of Poland: Warsaw, Poland, 2018.